



October 2008 Issue...

- 1** Segmentation – A Solution for the Future
- 3** Analysis of an Experimental Transformer Using PSCAD®
- 6** Simulation of Grid Connected Photovoltaic Systems
- 8** Investigation of Ferro-resonance Phenomena on a Station Service Transformer
- 12** Investigation of Harmonic Voltage Distortion During Capacitor Bank Switching due to System Resonance Issues and Transformer Saturation
- 15** Comparison of EMTDC™ based Simulation with Real Experimental Results of PV-AF System
- 19** Motivation for the Rest of Us
- 20** PSCAD® 2008 Training Sessions

Segmentation – A Solution for the Future

Dennis Woodford, P.Eng, Electranix Corporation

On the evening of August 14, 2003 I was in a hotel room in Denver, Colorado working on my laptop and in the background on the TV Larry King was interviewing Governor Gray Davis of California and Governor Bill Richardson of New Mexico. The topic of conversation was the North Eastern Blackout that had occurred that afternoon. Governor Davis had to deal with rotating blackouts in California and Governor Richardson had been the Secretary of Energy during the Clinton Administration. Their conclusion was “the electric power system requires firewalls.”

As I worked away, I was musing what would a firewall for an electric power system be? Then I realized that the firewall would be DC transmission. And indeed the Province of Quebec was buffered from the blackout because their interconnections to the blacked out region was through DC transmission links. Could DC firewalls be a practical solution to what Governors Davis and Richardson were concluding?

Others obviously thought so. DC Interconnect Inc. of Vancouver, BC understood the firewall capabilities of DC transmission. They worked with EPRI having Electranix as a subcontractor and with system models provided by the Midwest ISO (MISO), and segmented the Northeast North American power system into segments using about 30 back-to-back voltage sourced converters. A disturbance that precipitated a collapse of the power system similar to the August 14, 2003 event was developed without segmentation. The disturbance was repeated with segmentation and the results were a dramatic improvement. The disturbance did not propagate across the region.

In order for segmentation to be successful, the DC converters were modelled as voltage sourced converters, which provide AC voltage support at their terminals. The most important control feature was to modulate the power schedule through the DC link as a function of frequency difference between the networks on each side of the DC link. A simplified control concept illustrating this is shown in Figure 1.

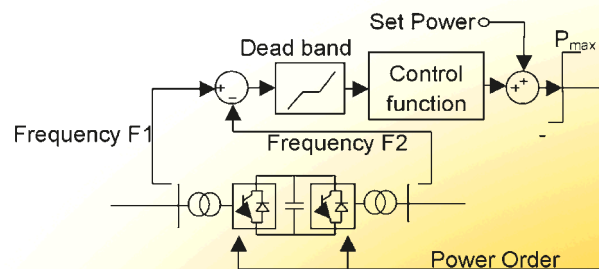


Figure 1 Segmentation controls for a back-to-back DC link.

If the frequency in one of the segments begins to fall because of a contingency, the DC links respond by increasing power flow to the distressed segment. In addition, because the frequency is allowed to fall further than it is possible with the system remaining synchronous, the governors of the generators can detect the frequency drop and respond more substantially to provide greater assistance.

The location of a DC segmentation converter at a congestion point will improve the transfer capacity of the transmission line it is connected to. Even a back-to-back DC converter located near the impedance centre has the potential to double the power

transfer through that transmission providing it is not thermally limited and can continue to provide AC voltage support at its terminals.

Another option to back-to-back DC transmission is GE's Variable Frequency Transformer (VFT). There is no reason VFTs could not be applied to achieve successful segmentation when AC voltage control is included if needed.

Greater gains in transfer capability can be achieved if the AC transmission line is converted to DC transmission over its full length and if the line is a long line (say several hundred kilometres). This can be achieved as a bipole with one conductor providing metallic return, or as a tripole that uses all three conductors to transmit power as shown in Figure 2. Here voltage sourced converters are considered for the simple reason they provide additional AC voltage support at the terminating busbars. Recently, it has become possible to apply voltage sourced converters (VSC) to overhead transmission lines using ABB's HVDC Light™ or Siemen's HVDC Plus™

The recent developments of voltage sourced converters to operate with overhead transmission, tripole, back-to-back VSCs and VFTs can be applied to achieve the benefits of segmentation that include substantial increases in reliability and transmission capability. All these can be modelled with precision on PSCAD® and with good representation on the standard power flow and stability programs. In some instances, models can be provided from the respective suppliers under confidentiality agreement.

Further Reading

- "Softening the Blow of Disturbances," H.K. Clark, A.A. Edris, M. El-Gasseir, K. Epp, A. Isaacs, D.A. Woodford, *IEEE Power and Energy Magazine*, January/February 2008.
- "Modelling and Dynamic Performance of a Rotary Power Flow Controller," Fujita, H., Ihara, S., Larsen, E.V., Pratico, E.R., Price, W.W., Power Engineering Society Winter Meeting, 2001, *IEEE*, Volume 2, 28 Jan-1 Feb, 2001, pp 599-604.
- "A New Multilevel Voltage-Sourced Converter Topology for HVDC Applications," Dorn, J., Huang, H., Retzmann, D., *CIGRE Paper No. B4-304*, 2008 CIGRE Technical Programme, Paris, August 2008.
- "Technical and Economic Aspects of Tripole HVDC," Barthold, L.O., PowerCon 2006, International Conference on Power System Technology, Chongqing, China, October 2006.
- "Application of HVDC Light to Power System Enhancement," Asplund, G., IEEE/PES Winter Meeting, Singapore, January 2000.

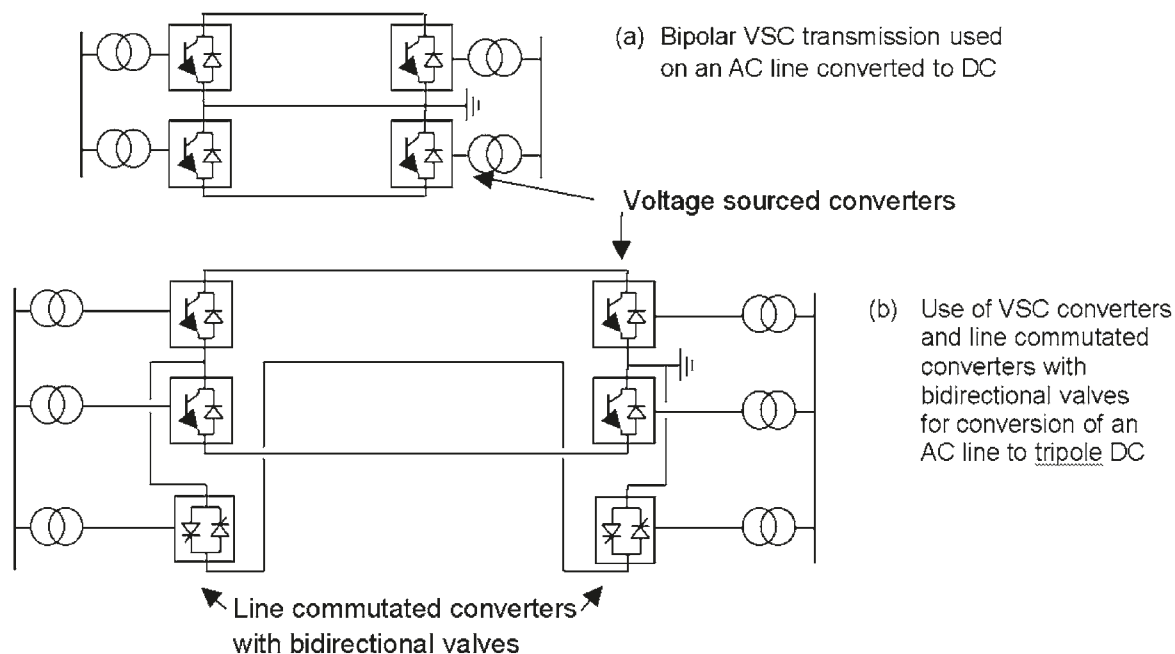


Figure 2 Conversion of AC transmission lines to DC using bipolar and tripolar converter configurations.

Analysis of an Experimental Transformer Using PSCAD®

KC Lewis, BE. (Elec)., Dip. Bus. Admin., Christchurch, New Zealand

The purpose of the study was to examine the theoretical performance of an experimental transformer, and to compare the PSCAD® results of the study with measurements taken from a 1 kVA model transformer. The transformer studied was a modified version of The Moving Coil Voltage Regulator. By varying the position of the moving coil, the output voltage of the transformer could be adjusted, as described by E T Norris, in 1937 [1].

In the case of the experimental transformer, the moving coil was replaced by two fixed coils, with the objective of simulating the moving coil by electronically controlling the currents in the fixed coils, and thus achieving similar results to that of the moving coil transformer.

The Moving Coil Voltage Regulator A brief comment on the characteristics of the moving coil regulating transformer could be helpful in understanding the desired performance of the experimental transformer. The moving coil transformer is essentially a single phase unit, but three can be combined to make a three phase bank.

It consists of two primary coils connected in series opposition on a long limb, with a movable short-circuited coil concentric with the primaries, and able to be moved the full length of the limb (Figure 1).

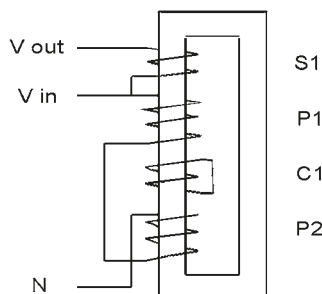


Figure 1 A schematic view of the Moving Coil Transformer.

As the moving coil traverses the length of the limb, the primary voltage is distributed across the primaries in a manner determined by it's position and coupling

with the individual primary winding. For example, when the coil C1 is concentric with primary P1, the full input voltage is developed across P2 (theoretically). Similarly, when the coil C1 is concentric with P2, the input voltage is developed across P1. Thus, a gradation of the input voltage from zero to the full value is distributed across the individual primary windings as the coil C1 moves over the length of the limb. In this way, the voltage developed across a secondary winding (not shown) coupled with a primary can be made to vary from zero to the full value, as determined by the turns ratio. Hence, the transformer output voltage can be regulated by moving the coil C1 to any desired position.

Transformers of this type have been built in a wide range of capacities and voltages. Many were installed in distribution systems, e.g. 11000 volts, 2000 kVA, three phase, would not be unusual. Some are still in service today even though they are very old. Because of the mechanical arrangement by which the moving coil is driven by a long lead screw, it is slow to respond to changes in the input voltage.

The Experimental Transformer The question was asked, could a regulating transformer be made that electronically simulated the effect of the moving coil, and not have the disadvantages of mechanical devices such as lead screws or tap changers, and hence have a fast response to changes in input voltage?

An experimental transformer was made by substituting the moving coil with two fixed windings, one each concentric with primaries P1 and P2 generally as shown in Figures 2 and 3.

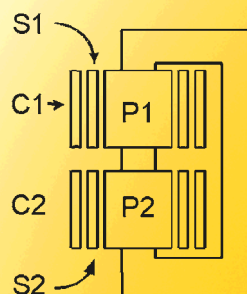


Figure 2 Transformer coil arrangement.

Two secondary windings S1 and S2 were included, also concentric with the primaries; the idea being that one could add and the other could subtract from the input voltage as desired. Winding S2 is not included in the calculations for the sake of simplicity.

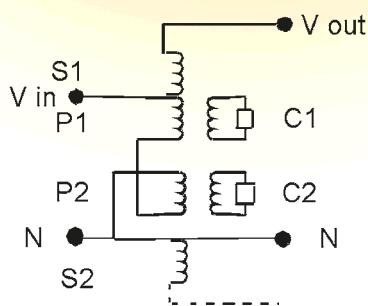


Figure 3 Transformer coil connections.

With this arrangement, if coil C1 is short-circuited, the effect is similar to the moving coil being concentric with P1; similarly, if C2 is short-circuited, the effect is similar to the moving coil being concentric with P2.

In the case of the moving coil regulator, the current flowing in the moving coil is the vector sum of a small current which will flow under no external load condition, plus a current due to the external load, as determined by the secondary/C1/C2 turns ratio. An equivalent current must flow distributed between the two fixed coils of the experimental transformer in such proportion as to have the same effect as if it was a moving coil.

The task was to control the currents in C1 and C2 so as to simulate the moving coil in intermediate positions along the limb. A successful method was devised to achieve this and careful measurements were taken of the transformer's performance over a range of conditions.

The 1 kVA, 240 volt, 50 hZ transformer was constructed using core stampings on hand; the arrangement generally as shown in Figure 4.

As the primaries are connected in opposition, the magnetic flux path is partially through iron and partially through air. Consequently, the magnetising current is considerably higher than for a conventional transformer of the same rating, due to the higher reluctance, but of a lesser proportion of harmonic content. Naturally, the flux distribution will vary from that shown, as currents in the windings are varied.

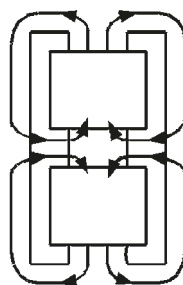


Figure 4 General arrangement.

Transformer circuit loop equations were written, solved, and the results compared with measured values; a rather tedious business. A more illustrative and educational approach was sought using PSCAD® as the tool.

PSCAD® Model A PSCAD® transformer model was developed by Support Services, Research and Support Engineer, Juan Carlos Garcia. This successfully produced good correlation with measured results found through experimentation. The model was subsequently modified by Dr. Neville Watson, at the University of Canterbury, New Zealand.

The PSCAD® model setup is shown in Figure 5. The PSCAD® model provides for calculations of voltage, currents and phase angles to be made at any point in the circuit as desired, and thus, allows a very good mental picture of the transformer behaviour to be gained as various input options are examined. It is simple to vary inputs.

...the inclusion of the phasor feature of PSCAD® enabled phase relationships between voltages and currents in the various windings to be displayed in graphic form for easy interpretation...

The visual presentation of inputs and outputs on screen is a superior educational way of understanding the behaviour of the device, as compared with looking at numbers only through calculation. The fast response of the system allows the effect of changes to the circuit or other input values to be seen quickly, as compared with obtaining the results by experiments with hardware.

Calculations using Matlab, PSCAD®, and measurement by experimentation with the transformer all agree, engendering confidence in the model. So, the PSCAD® transformer model has achieved the purpose for which it was developed; the analysis of an “oddball” transformer, in a clear and reliable manner.

Also, the model was used to simulate a “moving coil” transformer. Knowing the mutual inductance between coil C1 and the primary coils, and assuming linearity, values of mutual inductance between C1, P1 and P2 were calculated for a number of positions along the limb, on the basis that C1 moved from one end of the limb to the other. Using these values as input, here too, the PSCAD® model produced reliable output consistent with experiment.

The inclusion of the phasor feature of PSCAD® enabled phase relationships between voltages and currents in the various windings to be displayed in graphic form for easy interpretation.

Concluding Remarks The project was a success as the PSCAD® program produced results which correlated nicely with the experiment.

The use of the PSCAD® model has enabled the results of the transformer analysis to be displayed in the form of sinusoids and phasors, as well as in numerical data. These graphical presentations are a powerful visual aid to understanding the transformer behaviour to various inputs and a nice reward for the effort involved.

Because of the ease of use of the model, various design options can be investigated with confidence.

References:

[1] *The Journal of The Institution of Electrical Engineers.*
Volume 83. “The Moving Coil Regulator” by E T Norris.

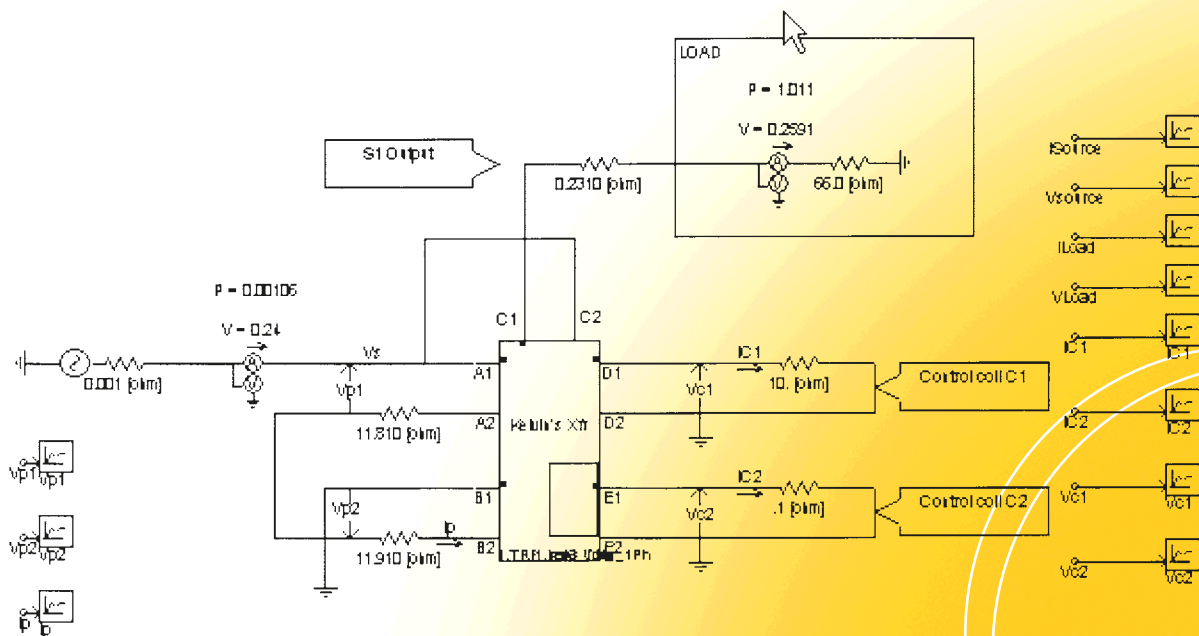


Figure 5 The PSCAD® model.

Simulation of Grid Connected Photovoltaic Systems

Athula Rajapakse, Department of Electrical and Computer Engineering, University of Manitoba, Winnipeg, Canada

Rising attention to distributed generation (DG) and green energy alternatives to conventional fossil fuel-based electricity has revived the interest in grid-connected photovoltaic (PV) systems. As the cost of PV has come down, applications such as building integrated PV systems are becoming increasingly popular [1]. When larger PV installations are designed, studies need to be performed at the power system level to examine the impacts of integration. For small scale distributed generation, interconnection standards, such as IEEE 1547 2003 [2] and local utility interconnection regulations define the grid interface requirements.

The protection is based on the philosophy that in case of grid disturbances (e.g. voltage drops or frequency deviation), distributed generators will be disconnected from the network immediately. The protection at the grid interface and the DG control must be designed to meet requirements. PSCAD®/EMTDC™ can be used for studies involving controller tuning, protection setting, power quality investigations and system validations among others [3].

PV Array Model A solar cell can be modelled using an electrical equivalent circuit that contains a current source anti-parallel with a diode, a shunt resistance and a series resistance as shown in Figure 1a. The DC current I_{gr} , generated when the cell is exposed to light, varies linearly with solar irradiance.

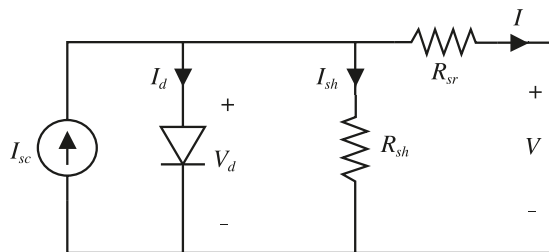


Figure 1a PV cell equivalent circuit.

The current I_d through the anti-parallel diode is largely responsible for producing the nonlinear I-V characteristics of the PV cell (Figure 1b).

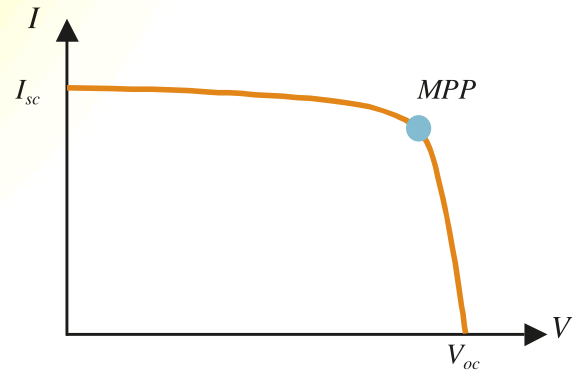


Figure 1b PV cell typical I-V characteristics.

The basic equation that characterizes the solar cell I-V relationship can be derived considering the equivalent circuit shown in Figure 1. The Kirchoff's current law provides

$$I = I_{sc} - I_d - I_{sh} \quad (1)$$

Substitution of relevant expressions for the diode current I_d and the shunt branch current I_{sh} yields

$$I = I_{sc} - I_o \left[\exp \left(\frac{V + IR_{sr}}{nkT_c/q} \right) - 1 \right] - \left(\frac{V + IR_{sr}}{R_{sh}} \right) \quad (2)$$

In (2) I_{sc} is the photo current and it is a function of the solar radiation on the plane of the solar cell G and the cell temperature T_c

$$I_{sc} = I_{scR} \frac{G}{G_R} [1 + \alpha_T (T_c - T_{cR})] \quad (3)$$

where I_{scR} is the short circuit current at the reference solar radiation G_R and the reference cell temperature T_{cR} . The parameter α_T is the temperature coefficient of photo current. The current I_o in (2) is called the dark current, a function of cell temperature only, and is given by

$$I_o = I_{oR} \left(\frac{T_c^3}{T_{cR}^3} \right) \exp \left[\left(\frac{1}{T_{cR}} - \frac{1}{T_c} \right) \frac{q e_g}{nk} \right] \quad (4)$$

where I_{or} is the dark current at the reference temperature. The other parameters appearing in (2)-(4) are the electron charge q , the Boltzmann constant k , the band-gap energy of the solar cell material e_g , and the diode ideality factor n .

All of the constants in the above equations can be determined by examining the manufacturer's specifications of the PV modules and published or measured I-V curves. A PV array is composed of series and parallel-connected modules and the single cell circuit can be scaled up to represent any series/parallel combination.

A PV cell model based on the above equations was implemented as a custom component in PSCAD®

Maximum Power Point Tracking The amount of power that can be drawn by a solar cell depends on the operating point on the I-V curve and the maximum power output occurs around the knee point of the curve. A maximum power point tracker (MPPT) is a power electronic DC-DC converter inserted between the PV array and its load to ensure that the PV module always operates at its maximum power point as the temperature, insolation and load vary. A popular MPPT algorithm based on the Incremental Conductance [4] method was implemented in PSCAD®

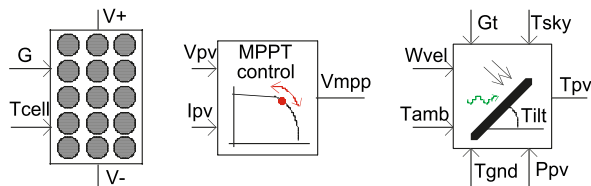


Figure 2 PV system simulation components library.

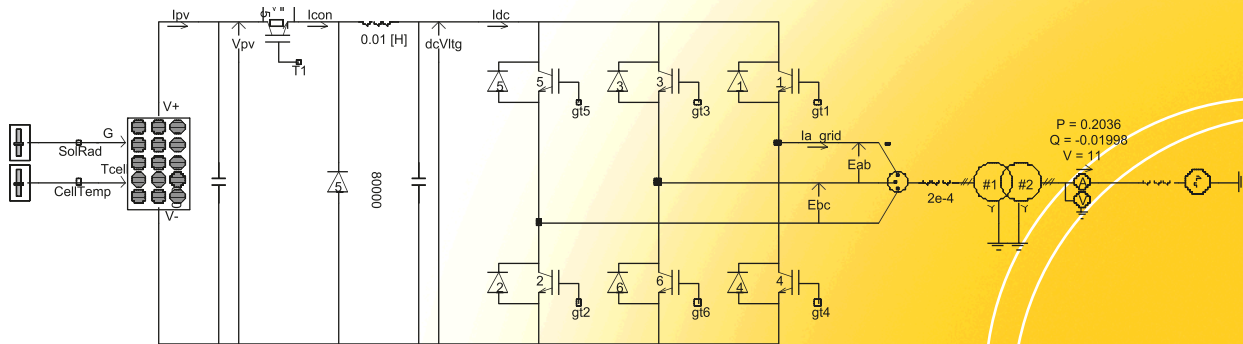


Figure 3 Example of simulating a grid connected PV system simulation.

Simulation of a Grid Connected PV Inverter

A simple example of using these components for a system study is shown in Figure 3. The external grid is represented by its Thevenin's equivalent. Basic blocks of the MPP Tracking control are shown in Figure 4.

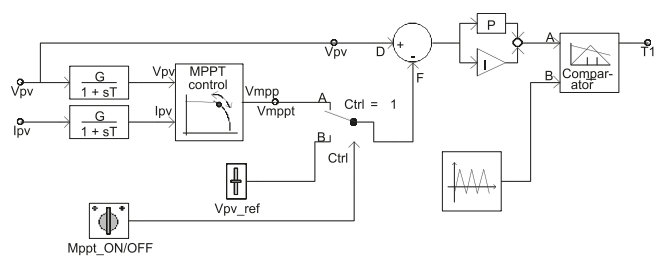


Figure 4 Simple DC-DC converter control with MMP tracking.

athula@ee.umanitoba.ca

References

- [1] Paul Maycock and Travis Bradford, "PV Technology, Performance, and Cost: 2007 Update Report," produced by Prometheus Institute for Sustainable Development and PV Energy Systems, Cambridge, MA, USA.
- [2] "IEEE Standard for Interconnecting Distributed Resources with Electric Power Systems," IEEE Standard 1547-2003.
- [3] A. D. Rajapakse, D. Muthumuni, N. Perera, and K. Strunz, "Electromagnetic Transients Simulation for Renewable Energy Integration Studies," Proceedings of IEEE PES Annual Meeting, Tampa, FL, USA, 24-28 June 2007.
- [4] Hussein K.H., Muta I., Hoshino T., Osakada, M., "Maximum Photovoltaic Power Tracking: An Algorithm for Rapidly Changing Atmospheric Conditions," Generation, Transmission and Distribution, IEE Proceedings-Volume 142 Issue 1, Jan. 1995, Pages: 59-64

Investigation of Ferro-resonance Phenomena on a Station Service Transformer

Nitus Voraphonpipit, Electricity Generating Authority of Thailand, Thailand (nitus.v@egat.co.th)
Dharshana Muthumuni, Manitoba HVDC Research Centre, Canada

This article describes ferro-resonance phenomena on a 12.5 MVA 230/7.2 kV station service transformer. The event took place during a black-start exercise at a power plant in Thailand. A switching operation of the power plant caused ferro-resonance leading to an abnormal level of noise and generally creating over-voltages which can lead to equipment failure. Field tests, analytical solutions and computer simulations were used to identify the problem and find solutions. After investigating a number of possible solutions, improvement of switching order was identified as the most effective.

Ferro-resonance is a non-linear oscillation phenomenon of a circuit consisting, at least, of a nonlinear inductance and a capacitance in series and supplied by an alternating current source. In the power system, it typically involves the non-linear magnetic inductance of a transformer and the capacitance of cables and transmission lines among others. The capacitance can also be the grading capacitances of a high voltage circuit breaker. Ferro-resonance is more likely in unloaded transformers and potential transformers where the resistive damping is minimal. In this case, the black start exercise of a 300 MW combined cycle power plant consisting of two 100 MW gas turbines (GT) and a 100 MW steam turbine (ST), was performed as described in [1].

The high voltage circuit breaker of the station service transformer was opened during the black start as a procedure. This high voltage circuit breaker was connected directly between the 230 kV main bus and the station service transformer. A very loud noise at the station service transformer followed after the 100 MW gas turbine was completely started-up and the generator circuit breaker was closed to energize the 230 kV main bus. Ferro-resonance was a possible cause of such loud noise. The over-voltage caused by ferro-resonance has the potential to damage the transformer and the surge arresters. Therefore, analysis and computer simulations were done and field tests carried out to find effective solutions.

Ferro-resonance Analysis The single line diagram of the power plant is presented in Figure 1. A high voltage circuit breaker (80142C) is shown in Figure 2.

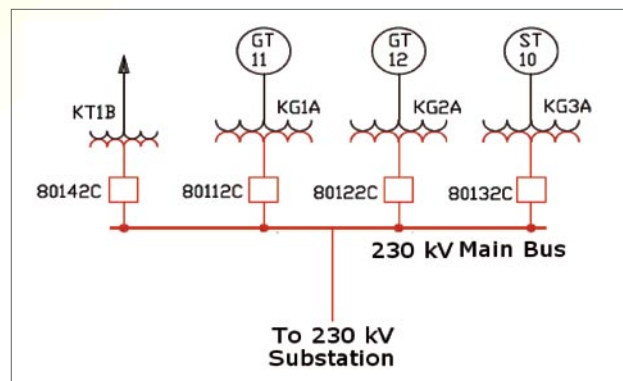


Figure 1 Single line diagram.



Figure 2 High voltage circuit breaker (80142C).

The station service transformer (KT2B), is a 230/7.2 kV oil type unit which has a capacity of 12.5 MVA (shown in Figure 3). During the black start exercise, the gas turbine unit no. 11 started up and reached a stable state. When the excitation system of the generator regulated the terminal voltage to the set-point, the generator circuit breaker (no. 80112C) was closed to energize the 230 kV main bus. At this point, the loud noise was heard near the transformer (KT2B).

Preliminary graphical analysis was used to analyze the operating condition of the transformer. Neglecting higher order harmonics in the voltage, the voltage-current characteristic (VI-curve) of the transformer (KT2B) and the grading capacitors could be presented as in Figure 4 [2-3]. The grading capacitors comprised of two capacitors connected in series (2,454 pF and 2,469.6 pF –values referred to secondary).



Figure 3 The station service transformer (KT2B).

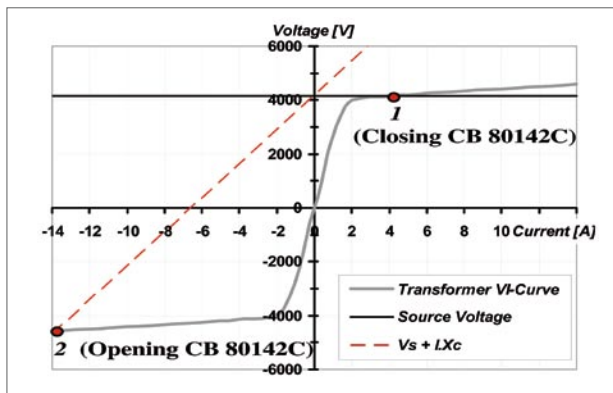


Figure 4 Graphical analysis.

In Figure 4, the intersection of the source voltage line and the VI-curve of the transformer (point 1) is the operating point of the transformer when the circuit breaker 80142C is closed.

The transformer was directly connected to the 230 kV main bus and the grading capacitors of the circuit breaker 80142C were shorted. When the circuit breaker 80142C was opened, the grading capacitor was effectively in the circuit. The circuit became a series connection of the grading capacitors and an unloaded transformer. The operating point was then moved to the third quadrant (point 2) where the VI-curve of the transformer and the VI-curve of source voltage pulse voltage across the grading capacitors ($V_s + I.X_c$) intersect. It can be seen from Figure 4 that ferro-resonance will occur whenever the 230 kV main bus is energized while the circuit breaker 80142C is opened.

However, the graphical analysis provided only approximate results. Voltage waveforms at the transformer terminal during the ferro-resonance event were of interest. Thus, computer simulations based on detailed electromagnetic transient programs (EMT) became necessary.

Simulation, Field Tests and Resolution

Ferro-resonance can be classified into four different modes, namely, the fundamental mode, sub-harmonic mode, quasi-periodic mode, and chaotic mode [4]. Graphical analysis cannot provide detailed voltage waveforms that characterize ferro-resonance. The single line diagram in Figure 1 was modelled on an Electromagnetic Transient Program (EMT) to analyze the ferro-resonance phenomena.

The PSCAD®/EMTDC™ program was selected as the simulation tool and a three-phase, three-limb Unified Magnetic Equivalent Circuit (UMEC) transformer model was used to model the transformer. This model correctly represents the core structure of the transformer under investigation and the accurate modelling of the core to account for phase coupling is a key requirement. The VI-curve of the transformer in Figure 4 was used as saturation data.

The field tests were conducted in July 2007. The measurement points were the three-phase secondary voltages of the transformer (KT2B). The power plant was shut down and started up by using the same switching sequence as explained earlier.

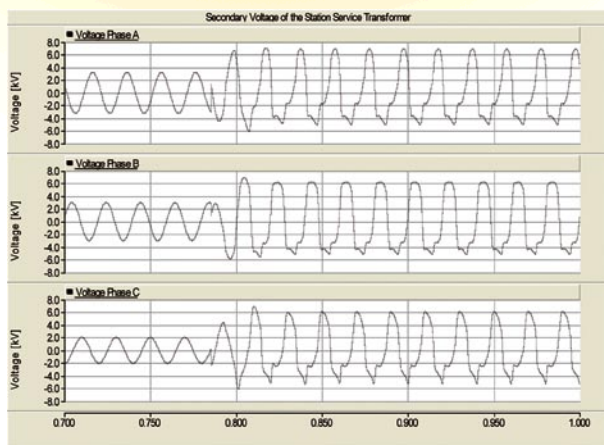


Figure 5 Simulation result (Tap No.5).

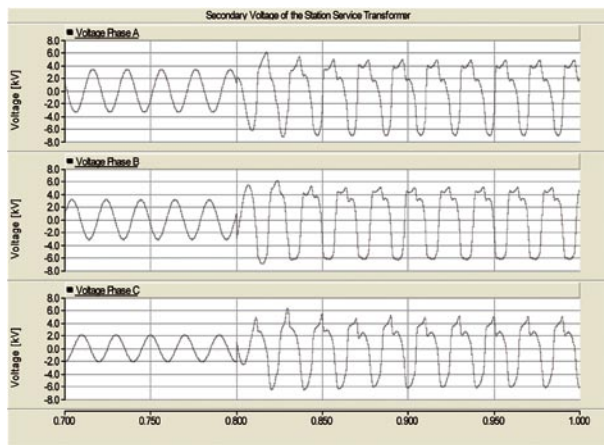


Figure 6 Simulation result (Tap No.10).

Field test results under two conditions are compared with simulation results in Figures 5-8. The simulation follows the field test results very closely. Computer simulations were used for further investigations.

The important factors found through computer simulations were that a detailed model of the transformer was significantly important to confirm the ferro-resonance phenomena. The initial voltage was important in order to match the field test results. Even though the magnitude of the voltage waveforms from the field test was not over the nominal voltage, it is impossible to state that the ferro-resonance phenomena would not present a risk for electrical equipment and that dangerous transient over-voltages would not occur after an event. Hence, the ferro-resonance phenomenon should be avoided and remedies should be investigated and proposed.

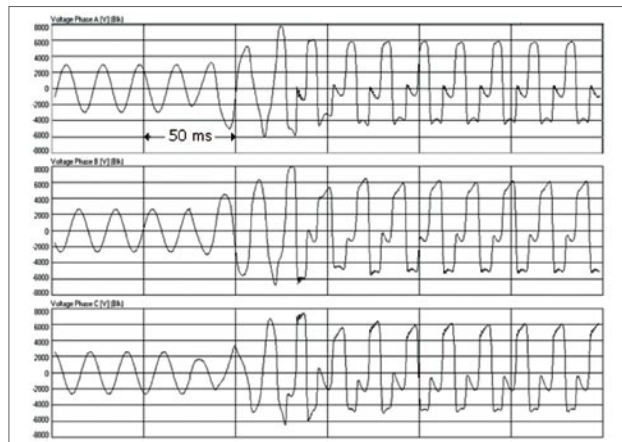


Figure 7 Field test result (Tap No.5).

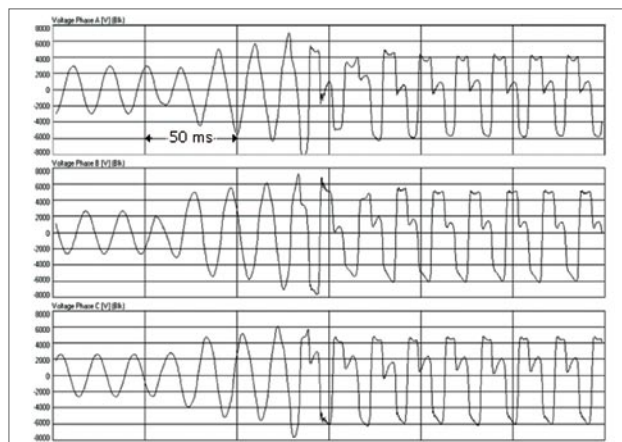


Figure 8 Field test result (Tap No.10).

*...the simulation follows the field test results very closely.
Computer simulations were used for further investigations...*

Three possible solutions were investigated:
1) Change the grading capacitors, 2) Connect resistive loads to the secondary of the transformer, and 3) Revised switching sequence. The first option was not cost effective and the second was not practical due to available plant area.

The third option became the most effective solution. The circuit breaker (80142C) shall not be opened during the black start or closed before energizing the 230 kV main bus. The black start was tested with the suggested switching sequence. Tests and simulations both confirmed an effective solution.

Conclusions There is a risk that ferro-resonance may occur during the black start process as the system has open circuit breakers and unloaded transformers. Even though graphical analysis can be applied to assess the risk of ferro-resonance, detailed modelling of the system on EMTP type programs are necessary to confirm the possibility and find solutions. Due to certain limitations and economic reasons, the addition of equipment to prevent the ferro-resonance may not be feasible. Guidelines on acceptable switching sequence that can prevent the ferro-resonance condition may be an efficient solution as it is in this case.

Acknowledgments The authors would like to thank the System Control and Operations Department and the Electrical Maintenance Section of Electricity Generating Authority of Thailand (EGAT) for the field tests and also Mr. Kittipon Chuangaroon for his consultation.

References

- [1] N. Voraphonpiput, "Ferro-resonance Phenomena of a Station Service Transformer during Black Start and Its Investigation," The 17th Conference of Electric Power Supply Industry (CEPSI 2008), Macau, China.
- [2] A. Greenwood, *Electrical Transients in Power Systems*, John Wiley & Sons, New York. 1991.
- [3] D. V. Razevig, *High Voltage Engineering*, Khanna Publisher, Delhi. 1996.
- [4] Ph. Ferracci, "Ferro-resonance," *Cahier technique* n° 190, Groupe Schneider, March 1998.

Investigation of Harmonic Voltage Distortion during Capacitor Bank Switching due to System Resonance Issues and Transformer Saturation

Jordan Sylvestre and Ken Burr, Distribution Performance Engineering, Manitoba Hydro

Voltage transients and high levels of voltage distortion were discovered by the Business Engineering Services unit of Manitoba Hydro, while investigating the complaints of two customers supplied from distribution station. Measurements conducted at the customers' plant recorded voltage distortion levels exceeding Manitoba Hydro's 5% limit (Figure 2). In addition, recordings also determined the customer is experiencing a 1.25 pu overvoltage associated with capacitor bank switching at the station. This 1.25 pu overvoltage was detected by an RPM recorder temporarily installed to monitor the system (Figure 1). During switching of banks CB71 and CB74 (Figure 4), their variable frequency drives (VFDs) intermittently trip on DC bus overvoltage protection.

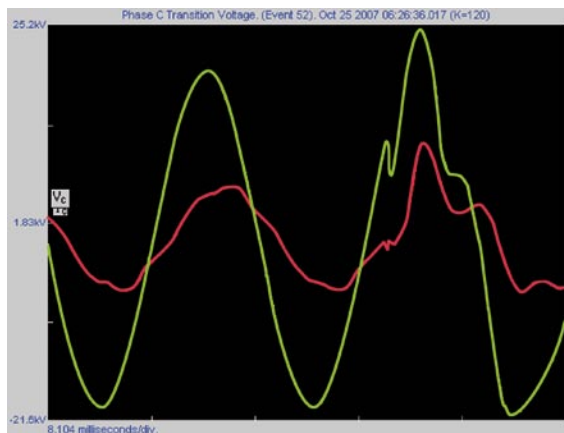


Figure 1 RPM plot obtained by the Business Engineering Services.

The distribution station has two shunt capacitor bank installations. CB74 is a 12.6 MVAR unit and CB71 is a 9.0 MVAR unit. The suspected cause of the high 5th harmonic voltage distortion is the switching of the larger CB74 bank.

A PowerVisa monitor was installed at Dawson Road Station to record capacitor switching events. The monitor was installed to capture data and confirm suspicions that CB74 is causing a parallel resonance around the 5th harmonic.

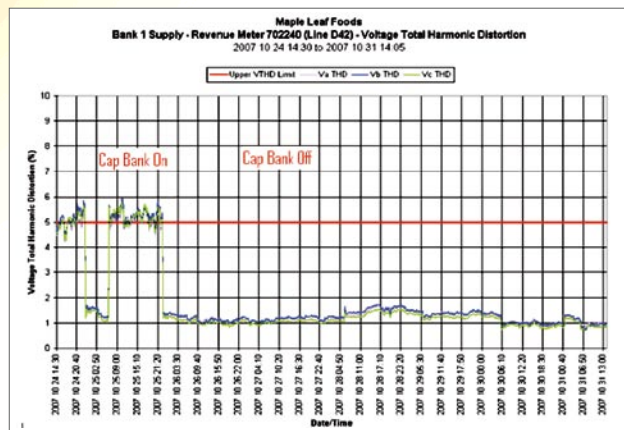


Figure 2 Voltage and THD limits at the customer site.

It has been calculated that switching on capacitors CB71 and CB74 results in a 2.5% and 4.1% voltage rise respectively. As a result, operational staff are reluctant to operate the CB74 breaker.

It can be seen from the data captured by the PowerVisa monitor in Figure 3 (during capacitor bank switching), that the 5th harmonic voltage increase is significantly higher with one capacitor bank on as opposed to the other. Due to the order of switching, the high voltage level is associated with the switching on of CB74.

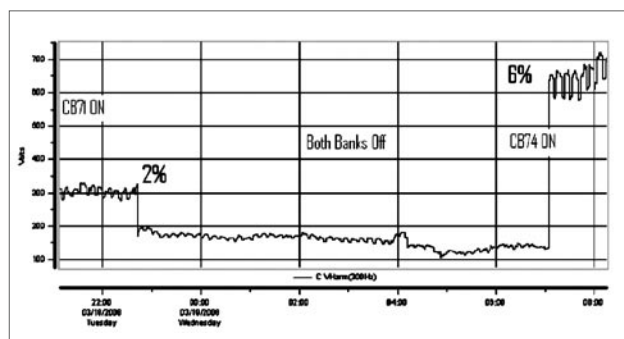


Figure 3 5th harmonic voltage recorded by PowerVisa recorder.

Alteration of the capacitor bank at CB74 is thus a necessary solution to ensure harmonic distortion along with voltage rise when the capacitors in service remain within acceptable limits.

Simulation Case Details A simplified model of Dawson Road Station was created using PSCAD®. Included in the model was a 66 kV source, a 66/24 kV delta-delta transformer, a grounding transformer, CB71 and CB74 and their associated capacitor banks, and a reactor at CB74.

A simulation was run for 100s with a solution time step of 100µs. Details of breaker state are as follows:

- 0s - CB71 closed, CB74 open
- 9s - CB71 ◇ open
- 11s - CB74 ◇ closed

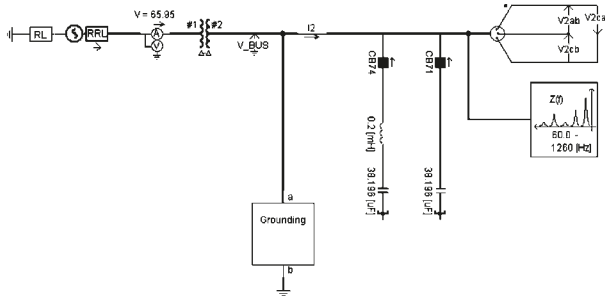


Figure 4 PSCAD® model of Dawson Road Station.

Results and Recommendations The results of the PSCAD® simulations confirmed field measurements. With CB74 (the larger bank) in service, the 5th harmonic voltage distortion was significantly higher than when CB71 was in service (the smaller bank).

An approximate 2% difference was seen in 5th harmonic voltage between the two capacitor banks. However, at Dawson Road, a 4% difference had previously been recorded. The possibility that this difference could be brought about by capacitor bank inaccuracy was then studied. It can be seen below (Figure 6) that looking at a value 10% lower than 12.6 MVAR (11.34 MVAR), the system is shifted closer to a 5th harmonic resonance.

It was found through simulation that the harmonic currents drawn by the grounding transformer (due to core saturation) causes the harmonic voltage amplification. However, changing this unit was not the cost effective solution. Hence, capacitor resizing was investigated, in an attempt to shift the system resonance points.



Figure 5 PSCAD® simulation with current CB74 bank.

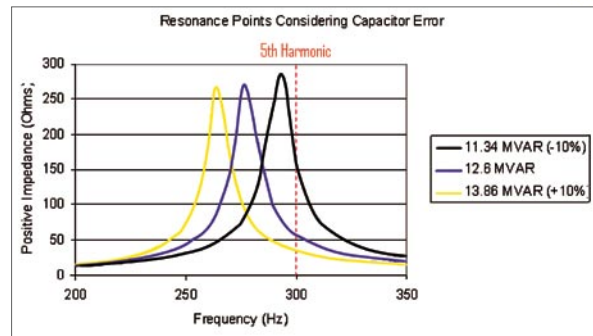


Figure 6 System proximity to 5th harmonic with CB74 bank manufacturing tolerance considered.

Figure 7 shows the system response with 11.34 MVAR at CB74, in which an 11% difference in capacitor bank responses was realized. Thus, it is likely that the capacitor bank at Dawson Road actually realizes a capacitance between 11.34 MVAR and 12.6 MVAR (manufacturing tolerance).

Following this determination, the impact of resizing capacitor bank CB74 was performed through frequency scan analysis. By looking at the system resonance points with varying combinations of CB71 and CB74 on and off, we arrive at Figure 8.

It can be seen that with only the 9.0 MVAR bank in service, no 3rd, 5th, or 7th harmonic resonance exists. Due to the fact that little harmonic voltages are seen when the 9.0 MVAR bank is in service, 9.0 MVAR is a good candidate for replacing the CB74 bank.

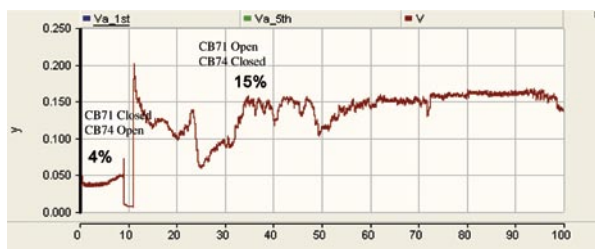


Figure 7 Results of a PSCAD® simulation run with 11.34 MV Ar capacitance at CB74.

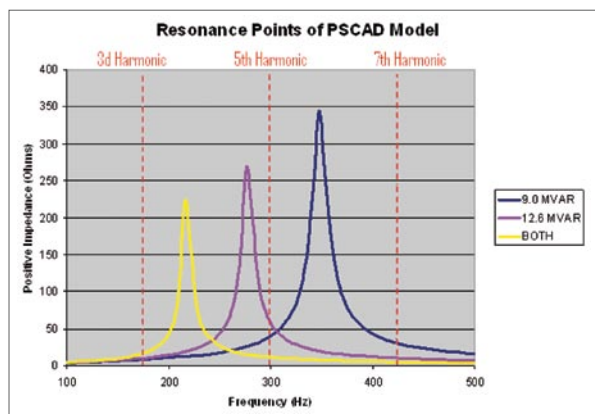


Figure 8 Resonance plots at the station.

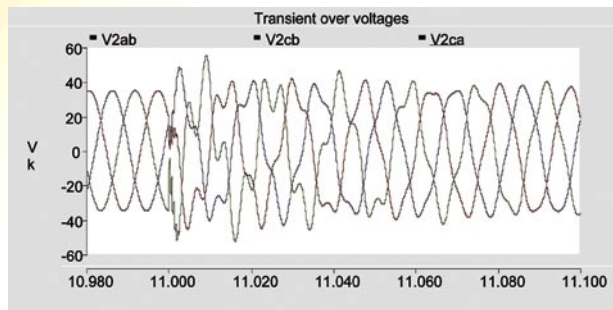


Figure 9 PSCAD® simulation of switching over-voltages at the station bus.

Conclusions In an attempt to improve power quality, the optimal size of capacitor banks was determined. Resizing the CB74 capacitor bank to 9 MVAR will address both the voltage rise and voltage distortion issues. The problem was amplified by the system resonance points interacting with the harmonic currents drawn by a saturating transformer. PSCAD® simulations were used to further verify field observations and to investigate mitigation methods.

Comparison of EMTDC™ based Simulation with Real Experimental Results of PV-AF System

Gyeong-Hun Kim, Hyo-Ryong Seo, Seong-Jae Jang, Sang-Soo Park, Minwon Park, In-Keun Yu, Changwon National University, Korea | Jin-Hong Jeon, Seul-Ki Kim, Chang-Hee Jo, Jong-Bo Ahn, Korea Electrotechnology Research Institute, Korea

This article presents comparison details of EMTDC™ based simulation and real experimental results of PV-AF system. The PV-AF system has not only an active filter function but also an anti-islanding function. For the purpose of accurate comparison, identical parameters are used for both the simulation and the real experiment. The simulation results based on PSCAD®/EMTDC™ agree very well with the experimental results.

Introduction to the PV-AF System The basic hardware configuration of the PV power generation system including the AF (Active Filter) function is very similar to the general PV power generation system. Including the AF function in the grid-connected PV power generation system would be very helpful for the improvement of power quality for individual consumers. Figure 1 shows the control block diagram of the PV-AF system.

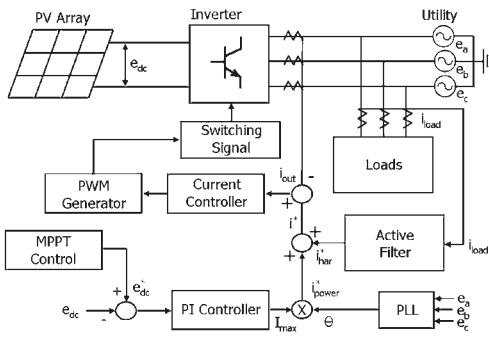


Figure 1 Control block diagram of the PV-AF system.

The PV-AF system also has the function of anti-islanding. Islanding occurs when a dispersed power generation system, is unintentionally operated alone when the utility has been disconnected. It may result in equipment damage or personnel safety hazards. The dispersed power generation system must have an anti-islanding function. There are two conventional anti-islanding protection methods: passive and active. The passive method has a non-detection zone and the active method has power quality problems. If the function of anti-islanding is included in the PV-AF system, it overcomes both these problems.

System Specifications Figure 2 shows the simulation circuit of hardware. Figure 3 shows the real hardware of the PV-AF system.

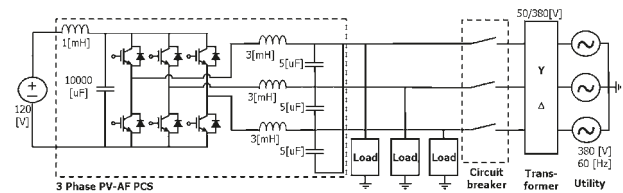


Figure 2 Circuit of the simulation and the real hardware.

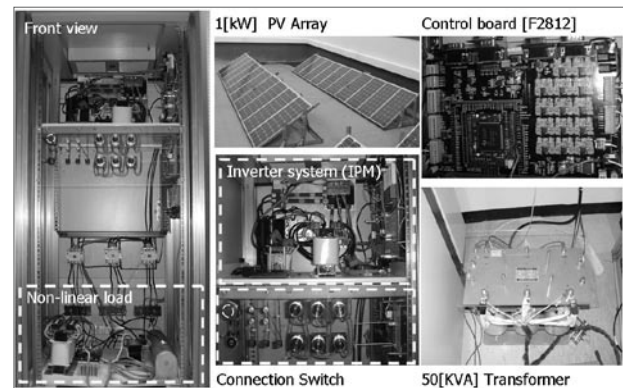


Figure 3 Real hardware of the PV-AF system.

Comparison Details of Simulation and Experimental Results In this article, two aspects were simulated and experimented. One is the active filter function, and the other is the anti-islanding function in the grid-connected PV-AF system.

A. Active filter function Figure 4 shows the circuit of the non-linear load and the hardware. A rectifier is used in this test. Figure 5 shows the utility current before compensating the harmonic current (pre-compensation). Figure 6 depicts the utility current of post-compensation. It shows that the inverter output current of EMTDC™ simulation result is equal to the real experimental result.

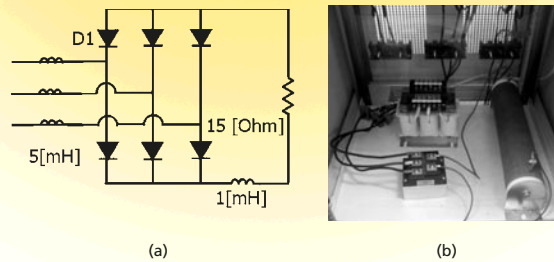


Figure 4 Non-linear load (a) rectifier (b) real hardware.

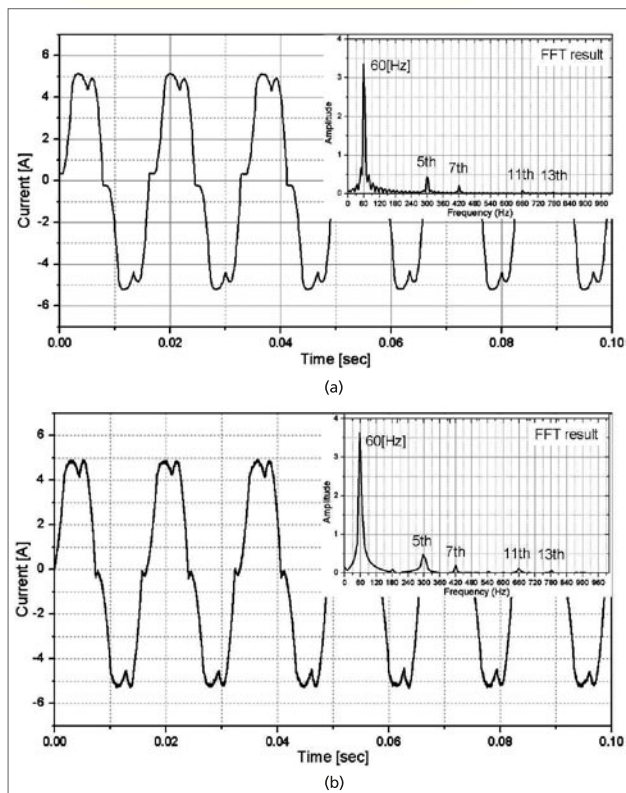


Figure 5 Utility current of pre-compensation (a) EMTDC simulation result (b) real experimental result.

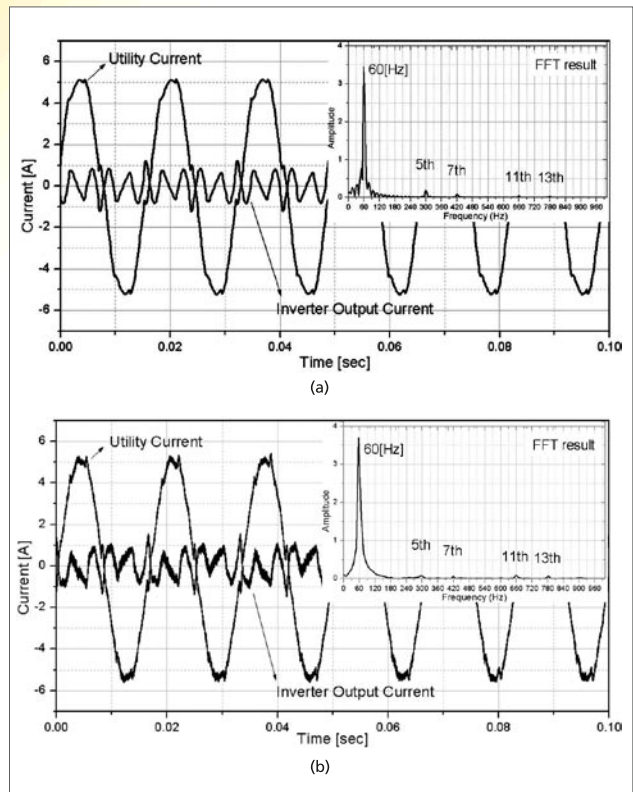


Figure 6 Utility current of post-compensation (a) EMTDC simulation result (b) real experimental result.

B. Anti-islanding function There are two cases in this test. One is a general PV power generation system without the active filter. In this case, the system doesn't have any anti-islanding method. The other is the PV-AF system with the anti-islanding function. Figure 7 shows RLC load for the test.

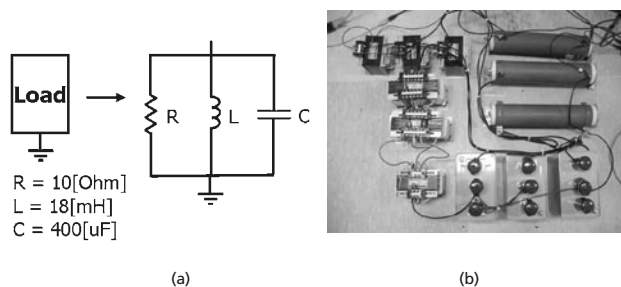


Figure 7 Loads for the islanding test (a) RLC load (b) real hardware.

$R = 10[\text{Ohm}]$
 $L = 18[\text{mH}]$
 $C = 400[\mu\text{F}]$

...to allow for accurate comparison, identical parameters were used in the simulation case and the actual setup. Experimental observations showed outstanding agreement with the simulation results from PSCAD®/EMTDC™.

Figure 8 demonstrates islanding occurring in the PV power generation system without active filter function. Although the utility system is disconnected, the system operates without interruption. The EMTDC™ simulation solution and the real experimental result are exactly the same in this case.

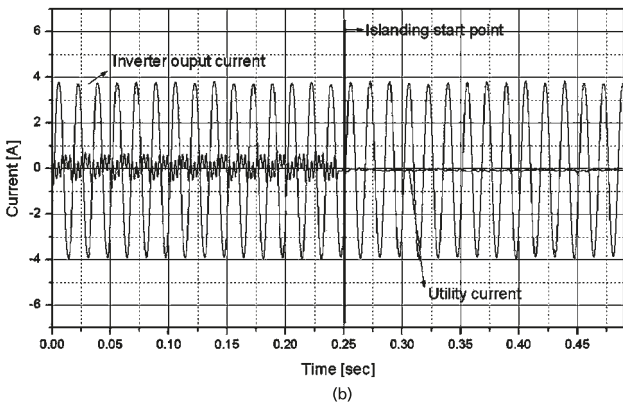
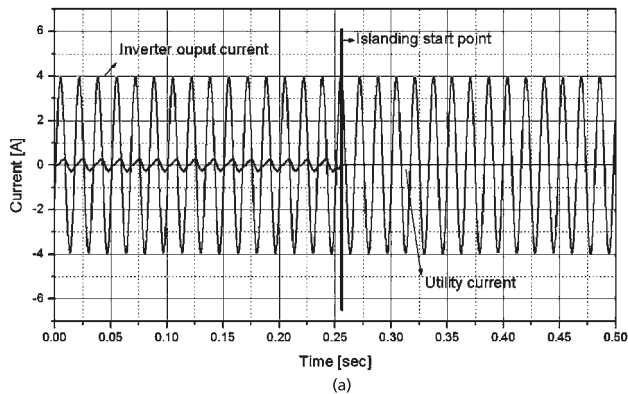


Figure 8 Utility current of pre-compensation (a) EMTDC™ simulation result (b) real experimental result.

Figure 9 shows that the islanding is protected by the PV-AF system. At the islanding instant, the utility system is disconnected and the inverter stops in 0.25[sec]. The EMTDC™ simulation result is very similar to the real experimental result.

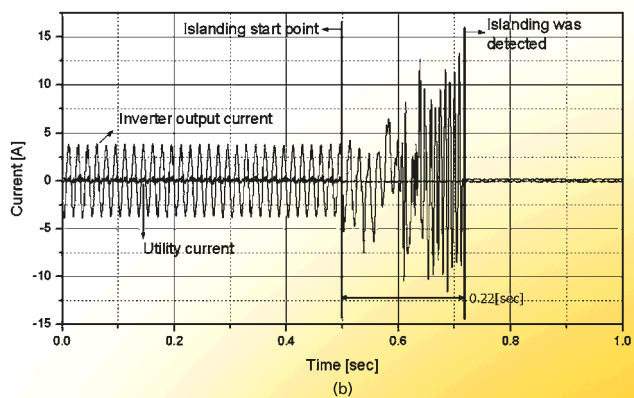
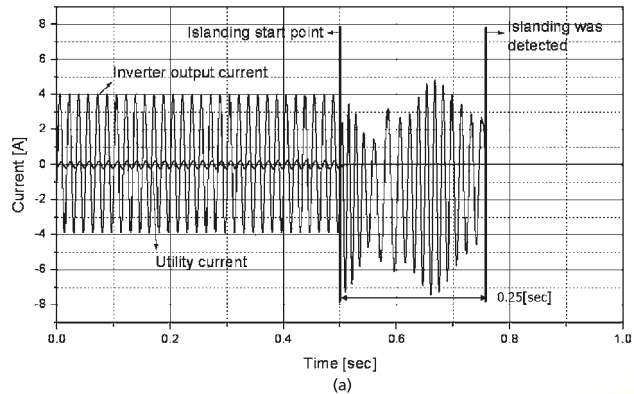


Figure 9 Utility current of pre-compensation (a) EMTDC™ simulation result (b) real experimental result.

In conclusion, the grid-connected PV-AF system was simulated in PSCAD®/EMTDC™, and was tested using the real hardware system under the same operational parameters.

1) The PV-AF system provides a novel anti-islanding function without any conventional anti-islanding method. It has neither the non-detection zone nor the power quality problem. Thus, it could improve power quality in the grid-connected PV power generation system.

2) The simulation results by PSCAD®/EMTDC™ coincide very well with the real experimental results; even the very complicated circuits and control schemes are used as depicted in Figure 10.

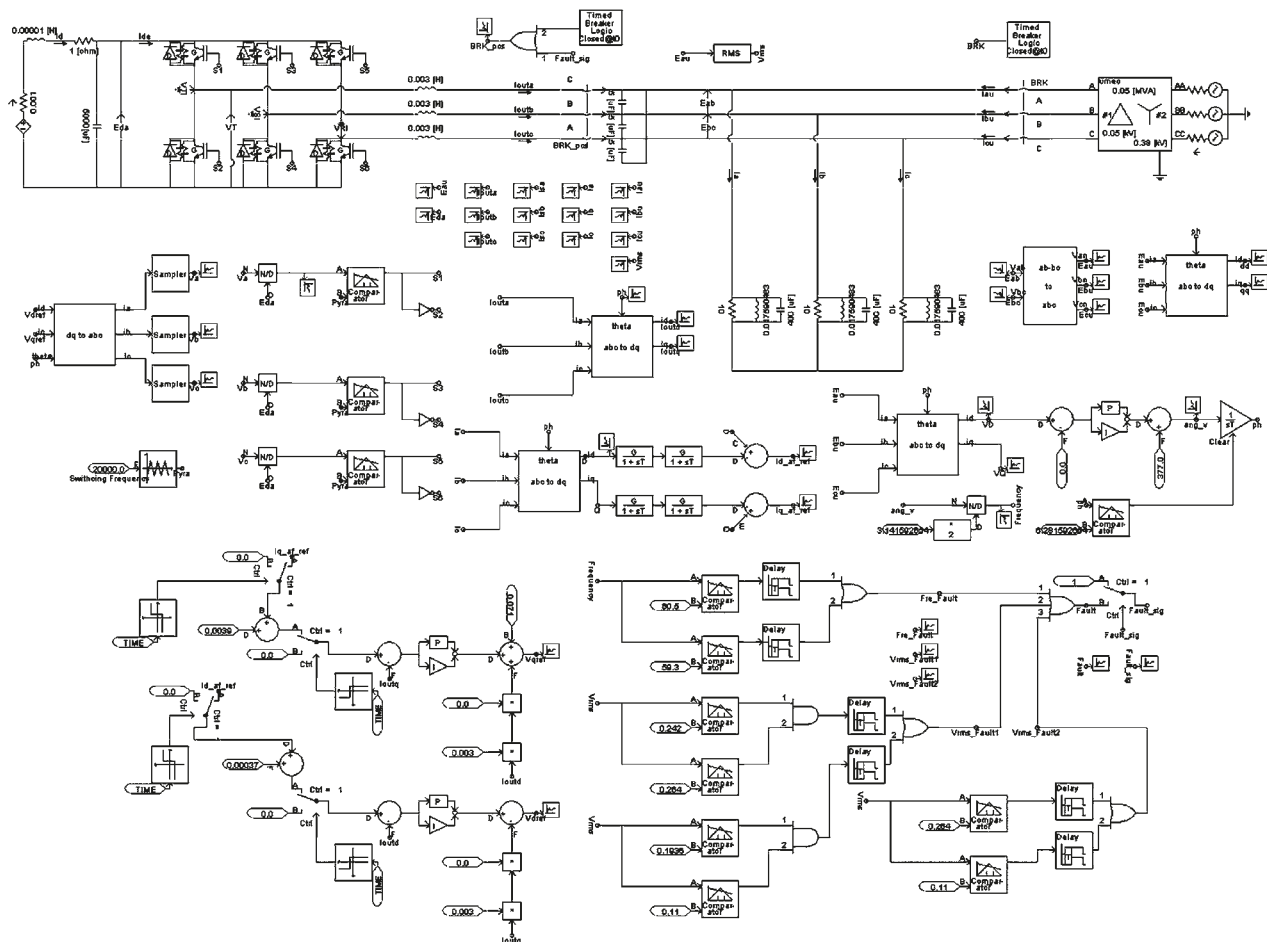


Figure 10 EMTDC™ simulation circuits.

Motivation for the Rest of Us

Paul Wilson, Manitoba HVDC Research Centre

The Manitoba HVDC Research Centre has been devoted to excellence since its founding in 1981 and our PSCAD® Development and PSCAD® Engineering Support teams are primary examples of this devotion. Through dedicated research and development in collaboration with leading institutions, we have introduced a variety of products and solutions, each a leader in its respective field.

We would like to take the opportunity to acknowledge our dedicated customers, partners and collaborators for your valuable input into our success. We value this in no small measure and are continuously striving to improve the products and services we offer to you. Our team of PSCAD®/EMTDC™ designers and engineers are implementing many new features and updating the simulation models to meet your future simulation requirements.

We understand from some of our users that PSCAD® is used to make Million dollar decisions. This realization humbles us and we recognize the stringent requirements for high quality this level of trust entails. Our users expect that we maintain our leadership in this domain of electromagnetic transient simulation. This singular fact motivates us to deliver solutions our users' trust.

With the introduction of our new website this summer, we provide one destination for comprehensive information on our products and services. This new site boasts additional PSCAD® client support through the new customer service portal which provides clients the ability to seek solutions to commonly asked questions. You can now renew maintenance and make purchases via our e-commerce portal.

Technical support and constant dialogue with our clients has long been crucial for driving our future development. We are very pleased to see you value our technical support immensely. The Technical Support team regularly receives high praise and appreciation for thorough and timely work. In an effort to maintain our high standards, we have more than doubled our technical support staff over the last three years. This group has the technical expertise in many different areas of simulation, modelling and application of electric power systems.

Please do not hesitate to contact them regarding your simulation concerns. They may help you in numerous ways:

- Review your PSCAD® simulation case
- Provide you with example simulations on a wide range of applications
- Share with you the many custom components that we have developed but not yet provided as Master Library components, to name a few,
 - Arc Furnace model, flicker and simulation examples
 - IGBT power loss and thermal calculation models
 - Solar cell model and example simulation
 - Single Phase Induction machine
- Discuss advanced simulation issues and issues related to new and emerging technology (Wind, PV, Solar)

Our support network includes our local representatives in various countries. These people are an extension of our technical support and sales groups and offer immediate services within their jurisdiction. We encourage you to work together with our representatives of your region. We strive to work with the very best—to provide you the best service.

Our Engineering Service Group has provided consulting services for over 20 years. Our unique position as developers of an industry standard simulation product gives us a competitive advantage in providing novel solutions. Such expertise has helped us provide innovative solutions to utilities, equipment manufacturers and various other sectors that had sought our expertise in the past. Some highlights include:

- Complex model development
 - Superconducting magnetic fault Current Limiter, Wind turbine models, Distribution level components
- AC transient studies
 - SSR studies, 500 kV line/ equipment rating design
- SVC and FACTS studies and commissioning work
- Voltage flicker simulation and analysis.

Our engineering study capability covers a wide range of areas including real time relay testing and detailed protection system analysis, HVDC, power quality, ship and locomotive systems, and many more. A more complete list is available on our website at www.pscad.com. We look forward to working with you in your efforts to find project efficiency and innovative engineering solutions.

Expanding Knowledge

The following courses are available, as well as **custom training courses** – please contact sales@pscad.com for more information.

Introduction to PSCAD® and Applications

Includes discussion of AC transients, fault and protection, transformer saturation, wind energy, FACTS, distributed generation, and power quality with practical examples. *Duration: 3 Days*

Advanced Topics in PSCAD® Simulation Training

Includes custom component design, analysis of specific simulation models, HVDC/FACTS, distributed generation, machines, power quality, etc. *Duration: 2–4 Days*

HVDC Theory & Controls

Fundamentals of HVDC Technology and applications including controls, modelling and advanced topics. *Duration: 4–5 Days*

AC Switching Study Applications in PSCAD®

Fundamentals of switching transients, modelling issues of power system equipment, stray capacitances/inductances, surge arrester energy requirements, batch mode processing and relevant standards, direct conversion of PSS/E files to PSCAD®. *Duration: 2–3 Days*

Distributed Generation & Power Quality

Includes wind energy system modelling, integration to the grid, power quality issues, and other DG methods such as solar PV, small diesel plants, fuel cells. *Duration: 3 Days*

Wind Park Modelling

Includes wind models, aero-dynamic models, machines, soft starting and doubly fed connections, crowbar protection, low voltage ride through capability. *Duration: 3 Days*

Industrial Systems Simulation & Modelling

Includes motor starting, power quality, capacitor bank switching, harmonics, power electronic converters, arc furnace, protection issues. *Duration: 1–2 Days*

Lightning Coordination & Fast Front Studies

Substation modelling for a fast front study, representing station equipment, stray capacitances, relevant standards, transmission tower model for flash-over studies, surge arrester representation and data. *Duration: 2 Days*

Modelling and Application of FACTS Devices

Fundamentals of solid-state FACTS systems. System modelling, control system modelling, converter modelling, and system impact studies. *Duration: 2–3 Days*

Connect with Us!

October 20–21, 2008

2008 CIGRE Canada

Conference on Power Systems

Winnipeg, Manitoba Canada

November 18–19, 2008

PSCAD® Applications Seminar

Wuhan, China

November 24–27, 2008

IEEE Conference on Sustainable Energy Technologies ICSET

Singapore

More events are planned! Please see www.pscad.com for more information.

PSCAD® Training Sessions

Here are a few of the training courses currently scheduled. Additional opportunities will be added periodically, so please see www.pscad.com for more information about course availability.

November 2008

HVDC Training Course

February 3–5, 2009

Introduction to PSCAD® and Applications

All training courses mentioned above are held at the Manitoba HVDC Research Centre Inc. Winnipeg, Manitoba, Canada
sales@pscad.com www.pscad.com

Please visit Nayak Corporation's website www.nayakcorp.com for courses in the USA.

November 2008

Introduction to PSCAD® and Applications

Princeton, New Jersey USA

For more information on dates, contact info@pscad.com today!

If you have interesting experiences and would like to share with the PSCAD® community in future issues of the *Pulse*, please send in your article to info@pscad.com